Journal of Nuclear Materials 386–388 (2009) 602–605

Contents lists available at ScienceDirect

Journal of Nuclear Materials

journal homepage: www.elsevier.com/locate/jnucmat

High temperature deformation of V-1.6Y-8.5W-(0.08, 0.15)C alloys

Tatsuaki Sakamoto [a,*], Hiroaki Kurishita [b], Sengo Kobayashi [a], Kiyomichi Nakai [a]

[a] Department of Materials Science and Biotechnology, Graduate School of Science and Engineering, Ehime University, Matsuyama 790-8577, Japan
[b] International Research Center for Nuclear Materials Science, Institute for Materials Research, Tohoku University, Oarai 311-1313, Japan

A B S T R A C T

In order to improve the high temperature strength of fine-grained and particle-dispersed V alloys, V-1.6Y-8.5W-0.08C and V-1.6Y-8.5W-0.15C (wt%) were fabricated by mechanical alloying and hot isostatic pressing, followed by annealing at 1000 and 1200 °C for 3.6 ks. Dispersoids of Y_2O_3, V_2C, WC and W_2C are detected by X-ray diffraction in the 1000 and 1200 °C-annealed specimens. Tungsten dissolves in the V matrix after annealing at 1200 °C. Tensile tests were performed at temperatures from 800 to 1100 °C at initial strain rates from 1.0×10^{-4} to 1.0×10^{-2} s^{-1}. The yield stress at 900 °C of 1200 °C-annealed V-1.6Y-8.5W-0.15C is approximately 2 times as high as that of V-4Cr-4Ti, due to combination of solution hardening by W and dispersion hardening by the dispersoids. The obtained stress exponent of plastic strain rate and activation energy for deformation suggest that the deformation of V-1.6Y-8.5W-0.08C and V-1.6Y-8.5W-0.15C is controlled by solute atmosphere dragging.

1. Introduction

Vanadium and its alloys are favorable for use in irradiation environments such as fusion reactor structural applications because of their inherently low-induced activation characteristics, large thermal stress factor and high fracture toughness prior to irradiation [1–3]. For their applications, however, it is required to improve the resistances to both radiation embrittlement and strength decrease at high temperatures.

Aiming at improving the resistances, the authors have studied neutron irradiation effects and high-temperature strengths for vanadium alloys with very fine grains and dispersed particles processed by powder metallurgical methods utilizing mechanical alloying (MA) and hot isostatic pressing (HIP) [4–8].

Regarding the high temperature strength, the alloys with fine dispersoids of Y_2O_3 and YN exhibit considerably higher yield strength below 900 °C than V-4Cr-4Ti (Nifs Heat-1) [2,9], but exhibit lower yield strength above 900 °C mainly due to grain boundary sliding [8]. In order to suppress such strength deterioration above 900 °C, we investigated solution hardening by Ti addition in V-1.7Y-2.1Ti [10] and V-2.3Y-4Ti-3Mo [11] alloys. However, the effect of Ti addition was found to be insufficient to improve the yield strength. Our recent studies showed that a V alloy containing V_2C dispersoid and W solute has a thermally very stable microstructure [7]. This result suggests that this alloy may exhibit improved strength above 900 °C. However, the high temperature deformation of the alloy has not been studied.

In this study, V alloys containing W solute and V_2C dispersoids were fabricated and the high temperature deformation behavior of the alloys has been investigated over wide temperature and strain rate ranges.

2. Experimental procedure

2.1. Specimens

Powders of pure V (0.106O, 0.0191N, in wt%), Y (1.39O, 0.052N), W (0.0150O, 0.0005N) and VC were used as the starting materials. They were mixed to provide nominal compositions of V-1.6Y-8.5W-0.4VC (V-1.6Y-8.5W-0.08C) and V-1.6Y-8.5W-0.8VC (V-1.6Y-8.5W-0.15C) in a glove box. The mixed powder and balls made of TZM (Mo-0.5Ti-0.1Zr) were charged into TZM milling vessels in the glove box with a purified H_2 gas (99.99999%). The vessels were subjected to MA with a three mutually perpendicular directions agitation ball mill for 216 ks in the H_2 atmosphere. The MA processed powder was enclosed in a mild steel capsule and HIPed at 1000 °C and 196 MPa for 10.8 ks in an Ar atmosphere. The details of the processing are reported elsewhere [6,7,11].

The as-HIPed compact was machined to prepare specimens for X-ray diffraction (XRD) analyses, microstructural observations by transmission electron microscopy (TEM) and energy dispersive X-ray spectroscopy (EDS) and tensile tests. All the specimens were wrapped with Zr and Ta foils and annealed at 1000 and 1200 °C for 3.6 ks in a vacuum of approximately 2.4×10^{-4} Pa. Thin foils for TEM were prepared by twin-jet electropolishing using a solution of 20 vol.% H_2SO_4 and 80 vol.% C_2H_5OH at approximately 5 °C and 40 V. Miniaturized tensile specimens had the dimensions

* Corresponding author.
E-mail address: sakamoto@eng.ehime-u.ac.jp (T. Sakamoto).

0022-3115/$ - see front matter © 2009 Elsevier B.V. All rights reserved.
doi:10.1016/j.jnucmat.2008.12.187

Table 1
Chemical compositions of the developed V alloys (mass%). The analysis methods are inductively coupled plasma atomic emission spectrometry for Y, W and Mo, infrared absorption spectrometry (using flame) for C and gaseous spectrometry for O and N.

	Y	W	Mo	C	N	O
V-1.6Y-8.5W-0.4VC	1.35	5.49	18.2	0.07	0.0145	0.188
V-1.6Y-8.5W-0.8VC	1.34	5.36	18.1	0.09	0.0135	0.217

Table 2
Microstructural parameters in V-1.6Y-8.5W-0.4VC, V-1.6Y-8.5W-0.8VC and V-2.4Y-3.4Mo.

	Average grain size (D/nm)	Average particle size (d/nm)	Number density ($r/10^{21}$ m^{-3})
V-1.6Y-8.5W-0.4VC	420	32	2.2
V-1.6Y-8.5W-0.8VC	410	30	3.5
V-2.4Y-3.4Mo	268	13.5	716

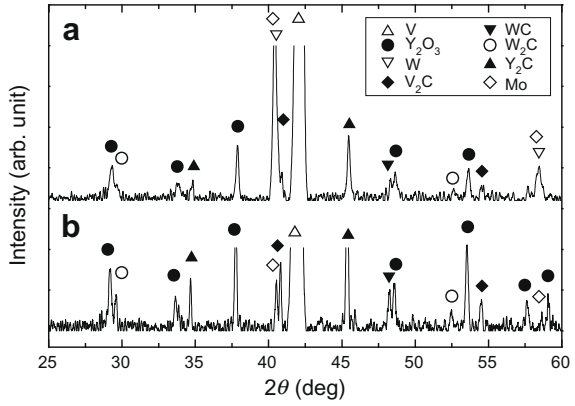

Fig. 1. X-ray diffraction profiles taken from V-1.6Y-8.5W-0.8VC after annealing at (a) 1000 and (b) 1200 °C for 3.6 ks.

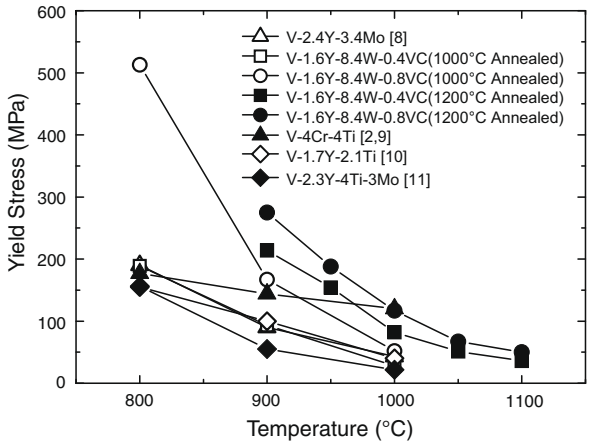

Fig. 3. Temperature dependences of yield stresses of various V alloys at the initial strain rate of 1×10^{-3} s^{-1}.

of 4.0 mm × 0.5 mm × 16 mm with the gage section of 1.2 mm × 0.5 mm × 5.0 mm [6].

Table 1 shows the chemical composition of the HIPed and annealed specimens of V-1.6Y-8.5W-0.4VC and V-1.6Y-8.5 W-0.8VC. The content of Mo is due to introduction of Mo debris from the TZM milling balls and vessels during MA.

2.2. Microstructures and tensile property evaluation

X-ray diffraction analyses were performed with Cu Kα radiation at 30 kV, 15 mA, a step angle of 0.01° and a scan speed of 0.03 deg/min. TEM observations were made by JEM-2000EX operating at 200 kV. Tensile testing was performed at temperatures from 800 to 1100 °C at initial strain rates from 1.0×10^{-4} to 1.0×10^{-2} s^{-1} in a vacuum better than 3×10^{-4} Pa. The details of the tests are described elsewhere [8].

3. Results and discussion

3.1. Microstructures

Fig. 1 shows XRD profiles of V-1.6Y-8.5W-0.8VC after annealing at 1000 and 1200 °C for 3.6 ks. For annealing at 1000 °C, peaks of V, W (Mo), Y_2O_3, V_2C, Y_2C, WC and W_2C are identified, as shown in Fig. 1(a), where the peaks of W and Mo are overlapped. After annealing at 1200 °C (Fig. 1(b)), the W peaks disappear and the V peak slightly shifts to a lower angle, indicating dissolution of W into the V matrix since the atomic size of W is larger than that of V. The disappearance of the W peak results in the distinct appearance of the Mo peak. Mo atoms do not dissolved into the V matrix because Mo atoms would be difficult to dissolve into the matrix during annealing due to the large size of Mo fragments introduced

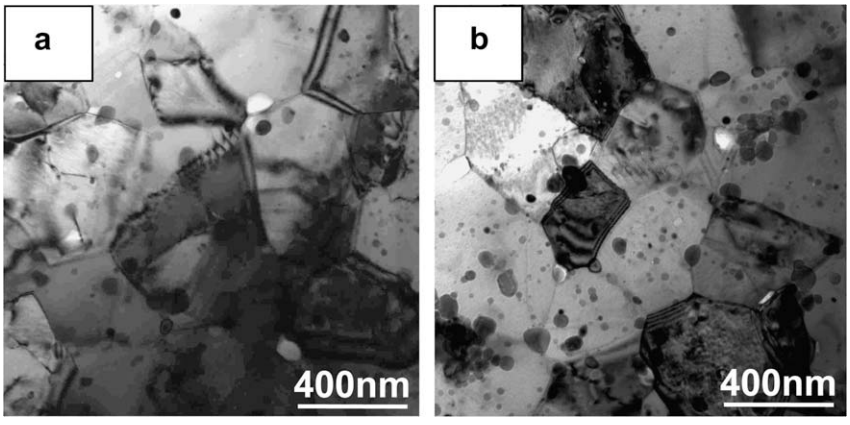

Fig. 2. Bright field images taken from (a) V-1.6Y-8.5W-0.4VC and (b) V-1.6Y-8.5W-0.8VC after annealing at 1200 °C for 3.6 ks.

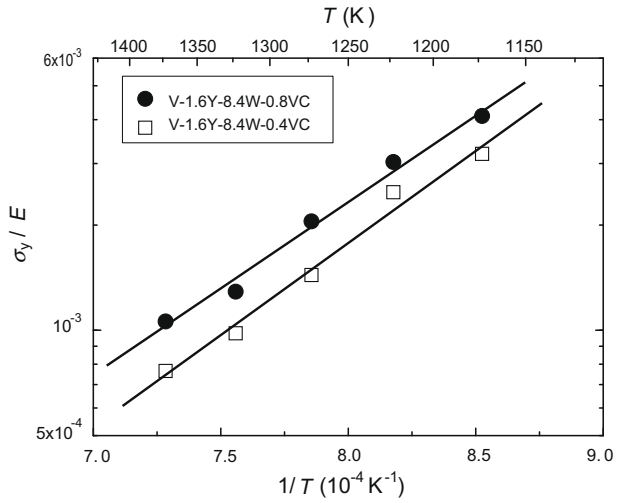

Fig. 4. Arrhenius plots of the yield stress normalized by the Young modulus at the initial strain rate of 1×10^{-3} s^{-1} in V-1.6Y-8.4 W-0.4 and -0.8VC after annealing at 1200 °C for 3.6 ks.

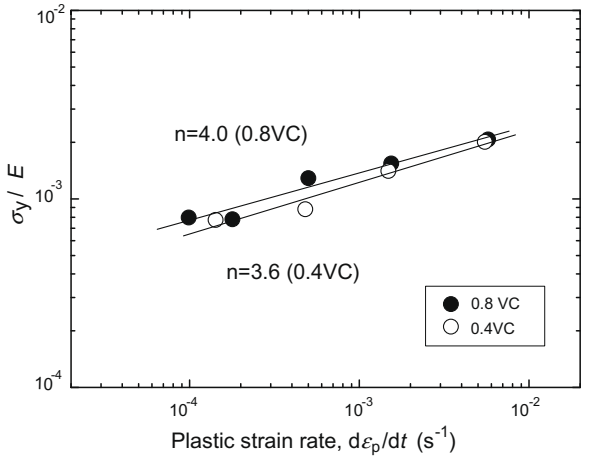

Fig. 5. Dependences of the yield stress normalized by the Young modulus on plastic strain rate at 1050 °C in V-1.6Y-8.4 W-0.4VC and -0.8VC after annealing at 1200 °C for 3.6 ks.

from the vessel and balls during MA. Contribution of Mo to solution hardening would be small.

Fig. 2 shows TEM bright field images taken from V-1.6Y-8.5W-0.4VC and -0.8VC annealed at 1200 °C. Many dispersoids of various sizes are observed inside the grains and at grain boundaries. The diameter of the dispersoids ranges from 8.2 to 130 nm for V-1.6Y-8.5 W-0.4VC and from 6.8 to 100 nm for V-1.6Y-8.5 W-0.8VC, with the average of 32 and 30 nm, respectively. The number densities of the dispersoids evaluated from the volume fraction and average diameter of the dispersoids were 2.2×10^{21} m^{-3} for V-1.6Y-8.5 W-0.4VC and 3.5×10^{21} m^{-3} for V-1.6Y-8.5 W-0.8VC. The average matrix grain diameter is 420 nm for V-1.6Y-8.5 W-0.4VC, and 410 nm for V-1.6Y-8.5W-0.8VC, which are considerably larger than that of V-2.4Y-3.4Mo (268 nm) [8] (Table 2).

EDS analysis showed that approximately 5%W dissolves in the matrix of the 1200 °C annealed specimen.

3.2. High temperature deformation

The test temperature dependence of the yield stress, σ_y, of the present alloys is shown in Fig. 3 together with those of other V alloys which we have reported so far. Here, the yield stress is defined as the 0.2% proof stress. The yield stresses of 1200 °C-annealed V-1.6Y-8.5 W-0.8VC and −0.4VC are considerably higher than those of 1000 °C-annealed V-1.6Y-8.5 W-0.8VC and -0.4VC. This is attributable to increased solution hardening by W. It should be noted that the yield stress of 1200 °C-annealed V-1.6Y-8.5 W-0.8VC is the highest in the temperature range of 900–1100 °C, and is approximately two times as high as that of V-4Cr-4Ti at 900 °C, This high strength of the alloy is attributable to the combination of solution hardening by W and dispersion hardening by the dispersoids. It should be noted that the dissolved W is more effective to hardening the matrix than the dispersoids because the yield stresses in V-1.6Y-8.5 W-0.8VC and -0.4VC alloys are larger than that in V-2.4Y-3.4Mo in spite of the smaller numbers of the dispersoids in V-1.6Y-8.5 W-0.8VC and -0.4VC alloys than that in V-2.4Y-3.4Mo.

Fig. 4 shows plots of the yield stress normalized by the Young's modulus (σ_y/E) in a logarithmic scale against the reciprocal of test temperature for V-1.6Y-8.5W-0.4VC and -0.8VC annealed at 1200 °C. Linear relationships are held up to 1100 °C for both alloys, with a nearly same slope. A noted feature for the present alloys is that there does not occur deviation of the linearity above 1000 °C which has always been observed so far in fine-grained V alloys [8] and which is attributable to grain boundary sliding.

Fig. 5 shows the double logarithmic plot of σ_y/E against plastic-strain rate at 1050 °C for V-1.6Y-8.5 W-0.8VC and -0.4VC annealed at 1200 °C. The plastic strain rate $\dot{\varepsilon}_p$ is estimated by

$$\dot{\varepsilon}_p = \dot{\varepsilon}_a(1 - (d\sigma/d\varepsilon_a)/K), \tag{1}$$

where $\dot{\varepsilon}_a$ and $d\sigma/d\varepsilon_a$ are the apparent strain rate (or the imposed strain rate) and work hardening rate, respectively, at the plastic strain of 0.2%. The value of K is the combined stiffness of the machine assembly including the specimen. The plot shows a linear relationship and the following relationship is hence held

$$\dot{\varepsilon}_p \propto (\sigma_y/E)^n, \tag{2}$$

where n is the stress exponent. The n values in V-1.6Y-8.5W-0.4VC and -0.8VC are 3.6 and 4.0 at 1050 °C, respectively, as listed in Table 3. It is known that the n value of alloys which exhibit large solution hardening is approximately 3 and increases with decreasing the contribution of solution hardening to the flow stress of the alloys. In addition, in view of difference in the number density of the dispersoids between V-1.6Y-8.5W-0.4VC and -0.8VC, we can say that the present result on the n value may reflect that the contribution of dispersion strengthening to the yield stress increases and that of solute atmosphere dragging decreases as the addition of VC increases.

From the above results of the strain rate and temperature dependence of σ_y/E, the rate equation for deformation of V-1.6Y-8.5 W-0.4VC and -0.8VC can be expressed by

$$\dot{\varepsilon}_p = A(\sigma_y/E)^n \exp(-Q/RT), \tag{3}$$

where Q is the activation energy for deformation, A is a constant, R the gas constant and T the absolute temperature. Eq. (3) can be rewritten into

$$ln(\sigma_y/E) = Q/nRT + (\ln\dot{\varepsilon}_p - \ln A)/n. \tag{4}$$

From Eq. (4) and the results shown in Figs. 4 and 5 the activation energy values for deformation in the temperature range 900–1100 °C in V-1.6Y-8.5 W-0.4VC and -0.8VC were determined to be 350 and 380 kJ/mol, respectively. The activation energy values are larger than the activation energy for self-diffusion in pure

Table 3
Tensile-test temperature, n value (stress exponent) and apparent activation energy for deformation in V-1.6Y-8.5 W-0.4VC and -0.8VC after annealing at 1200 °C.

	Test temperature (°C)	n	Q (kJ/mol)
V-1.6Y-8.5W-0.4VC	1050	3.6	350
V-1.6Y-8.5W-0.8VC	1050	4.0	380

V (300 kJ/mol) [12] and close to that of interdiffusion of W in V (357–393 kJ/mol) [13]. This suggests that the deformation controlling mechanism is solute atmosphere dragging of W. The higher activation energy for V-1.6Y-8.5W-0.8VC than for V-1.6Y-8.5W-0.4VC may be attributed to the larger contribution of dispersion hardening, as indicated by the comparison of the n value [14].

4. Conclusions

The high temperature deformation behavior of fine-grained and particle-dispersed V alloys containing W solute and V_2C dispersoids has been investigated. V-1.6Y-8.5W-0.4VC and −0.8VC (wt%) alloys were fabricated by MA and HIP processes and subjected to XRD analyses, TEM observations, and tensile tests at temperatures from 800 to 1100 °C at initial strain rates from 1.0×10^{-4} to 1.0×10^{-2} s^{-1}. The results were compared with those for V-4Cr-4Ti (Nifs Heat-1) and V alloys that we have investigated so far. The main results obtained are as follows.

1. V-1.6Y-8.5W-0.4VC and -0.8VC contain dispersoids of Y_2O_3, V_2C, Y_2C, WC and W_2C. The average diameters and number densities of the dispersoids are 32 nm and 2.2×10^{21} m^{-3} for V-1.6Y-8.5W-0.4VC and 30 nm and 3.5×10^{21} m^{-3} for V-1.6Y-8.5W-0.8VC, respectively. The average grain sizes for V-1.6Y-8.5W-0.4VC and -0.8VC are 420 and 410 nm, respectively. W dissolves in the V matrix after annealing at 1200 °C.
2. The yield stress of 1200 °C-annealed V-1.6Y-8.5W-0.8VC is the highest in the temperature range of 900–1100 °C and is approximately two times as high as that of V-4Cr-4Ti at 900 °C because of combination of solution hardening by W and dispersion hardening by the dispersoids.
3. The stress exponent of yield stress, n, at 1050 °C, in V-1.6Y-8.5W-0.4VC and -0.8VC are 3.6 and 4.0, respectively. This result indicates that the contribution of dispersion strengthening to the yield stress increases and that of solute atmosphere dragging decreases as the addition of VC increases.
4. The activation energies for deformation in V-1.6Y-8.5W-0.4VC and −0.8VC annealed at 1200 °C are 350 and 380 kJ/mol, respectively, in the temperature range 900–1100 °C. These values are close to that of interdiffusion of W in V (357–393 kJ/mol). This suggests that the high temperature deformation is controlled by solute atmosphere dragging of W in the alloys.

Acknowledgements

The authors would like to express their gratitude to Dr S Matsuo for his assistance for preparing the specimens and for his review of the paper. A part of this work was performed at International Research Center for Nuclear Materials Science, Oarai, and this work was partly supported by NIFS Budget Code NIFS05KFRF022, which is greatly appreciated.

References

[1] R.J. Kurtz, K. Abe, V.M. Chernov, D.T. Hoelzer, H. Matsui, T. Muroga, G.R. Odette, J. Nucl. Mater. 329–333 (2004) 47.
[2] T. Muroga, T. Nagasaka, K. Abe, V.M. Chernov, H. Matsui, D.L. Smith, Z.-Y. Xu, S.J. Zinkle, J. Nucl. Mater. 307–311 (2002) 547.
[3] T. Muroga, M. Gasparotto, S.J. Zinkle, Fus. Eng. Des. 61&62 (2002) 13.
[4] T. Kuwabara, H. Kurishita, M. Hasegawa, J. Nucl. Mater. 283–287 (2000) 611.
[5] H. Kurishita, T. Kuwabara, M. Hasegawa, S. Kobayashi, K. Nakai, J. Nucl. Mater. 343 (2005) 318.
[6] T. Kuwabara, H. Kurishita, M. Hasegawa, Mater. Sci. Eng. A 417 (2006) 16.
[7] H. Kurishita, T. Kuwabara, M. Hasegawa, Mater. Sci. Eng. A 432 (2006) 245.
[8] S. Oda, H. Kurishita, Y. Tsuruoka, S. Kobayashi, K. Nakai, H. Matsui, J. Nucl. Mater. 329–333 (2004) 462.
[9] T. Muroga, T. Nagasaka, A. Iiyoshi, A. Kawabata, S. Sakurai, M. Sakata, J. Nucl. Mater. 283–287 (2000) 711.
[10] H. Kurishita, S. Oda, S. Kobayashi, K. Nakai, T. Kuwabara, M. Hasegawa, H. Matsui, J. Nucl. Mater. 367–370 (2007) 848.
[11] T. Sakamoto, H. Kurishita, S. Kobayashi, K. Nakai, H. Arakawa, H. Matsui, Mater. Trans. 47 (2006) 2497.
[12] J.F. Murdock, C.J. McHargue, Acta Metall. 16 (1968) 493.
[13] J. Pelleg, V. Segel, Phys. B 393 (2007) 259.
[14] H. Yoshinaga, in: T. Suzuki (Ed.), Dislocation Dynamics, Syokabou, Tokyo, 1985, p. 189.